

Boron Clusters

International Edition: DOI: 10.1002/anie.201609766

German Edition: DOI: 10.1002/ange.201609766

Structure and Fluxionality of B_{13}^+ Probed by Infrared Photodissociation Spectroscopy

Matias R. Fagiani, Xiaowei Song, Petko Petkov, Sreekanta Debnath, Sandy Gewinner, Wieland Schöllkopf, Thomas Heine,* André Fielicke,* and Knut R. Asmis*

Abstract: We use cryogenic ion vibrational spectroscopy to characterize the structure and fluxionality of the magic number boron cluster B_{13}^+ . The infrared photodissociation (IRPD) spectrum of the D_2 -tagged all- ^{11}B isotopologue of B_{13}^+ is reported in the spectral range from 435 to 1790 cm^{-1} and unambiguously assigned to a planar boron double wheel structure based on a comparison to simulated IR spectra of low energy isomers from density-functional-theory (DFT) computations. Born–Oppenheimer DFT molecular dynamics simulations show that B_{13}^+ exhibits internal quasi-rotation already at 100 K. Vibrational spectra derived from these simulations allow extracting the first spectroscopic evidence from the IRPD spectrum for the exceptional fluxionality of B_{13}^+ .

Boron is electron-deficient and therefore has a strong tendency to share electrons. Consequently, pure boron compounds can exhibit pronounced delocalized bonding and aromatic behavior. These unusual electronic properties of elemental boron lead to a rich polymorphism.^[1] Bulk boron prefers three-dimensional structures based on deltahedral, mainly icosahedral or octahedral, subunits. Various boron nanostructures including nanosheets, nanotubes, nanoribbons and nanospheres with similar and sometimes superior properties as their carbon-based analogues have been predicted.^[2] Experimentally, only the synthesis of single- and multi-wall boron nanotubes has been reported.^[3] Larger boron clusters in the gas phase can adopt aromatic fullerene-like structures. The smaller clusters prefer planar, quasi-planar or cylindrical geometries with a charge-state dependent 2D to 3D transition at $n = 16$ for cations and $n = 39$ for anions.^[4] Since the first mass spectrometric experiments on boron clusters by Anderson and co-workers, B_{13}^+ has been known to be particularly stable and

unreactive.^[5] However, its structure remained subject to debate for some time.^[6] While the results from theoretical methods have converged and now predict a planar C_{2v} global minimum energy geometry consisting of an inner triangle surrounded by a ten-membered external ring, its spectroscopic verification has remained open.^[7] The special stability of this C_{2v} structure has been explained by its σ - and π -aromaticity.^[7–8] As a result of the delocalized bonding it is predicted to exhibit a very small barrier (0.4 $kJ\ mol^{-1}$) towards the internal rotation of the inner B_3 ring and has hence been termed a “molecular Wankel motor”, but this awaits experimental verification.^[9] Here, we use cryogenic ion vibrational spectroscopy in combination with density-functional-theory (DFT) computations and Born–Oppenheimer molecular dynamics (BOMD) simulations to characterize the structure and fluxionality of cold, mass-selected B_{13}^+ clusters in the gas phase, providing the first experimental evidence for internal quasi-rotation in B_{13}^+ already at very low temperatures.

In contrast to the wealth of experimental work on pure carbon clusters, spectroscopic studies on pure boron clusters are scarce and have predominantly focused on negative ions. Wang and co-workers have applied anion photoelectron spectroscopy (APS) in their pioneering work on boron anions up to B_{40}^- . With computational support from the Boldyrev group they were able to show that up to $n = 36$ boron cluster anions adopt planar or quasi-planar structures.^[8,10] Recently, they reported the first experimental evidence for a 3D cage structure, a so-called borospherene, for B_{40}^- , the smallest all-boron fullerene.^[10] Subsequently, they found evidence that B_{39}^- , another member of the borospherenes, is chiral.^[4c] In principle, APS accesses the neutral manifold, but it is limited by Franck–Condon considerations to probe structures that are similar to that of the anion ground state. More direct experimental information on the structure of neutral boron clusters has been limited to B_{11} , B_{16} and B_{17} , which have been probed by IR/vacuum-UV two color ionization experiments.^[11] These experiments confirmed the (quasi-)planar structures found by APS. The only experimental information on the structure of the cationic boron clusters B_n^+ comes from ion mobility measurements combined with a genetic algorithm search of low energy structures from Kappes, Ahlrichs and co-workers.^[4b] Their experimental collision cross section for B_{13}^+ is in agreement with that of the predicted global minimum energy C_{2v} structure (isomer **I** in Figure 1). However, an energetically substantially higher lying non-planar isomer (isomer **IV** in Figure 1) exhibits a nearly identical collision cross section, calling for a more definitive, spectroscopic identification. Moreover, the vibrational spectrum of B_{13}^+ does not only allow assigning its structure unambigu-

[*] M. R. Fagiani, Dr. X. Song, Dr. P. Petkov, S. Debnath, Prof. T. Heine, Prof. K. R. Asmis
Wilhelm-Ostwald-Institut für Physikalische und Theoretische Chemie, Universität Leipzig
Linnéstrasse 2, 04103 Leipzig (Germany)
E-mail: thomas.heine@uni-leipzig.de
knut.asmis@uni-leipzig.de

M. R. Fagiani, Dr. X. Song, S. Debnath, S. Gewinner, Dr. W. Schöllkopf
Fritz-Haber-Institut der Max-Planck-Gesellschaft
Faradayweg 4–6, 14195 Berlin (Germany)

Dr. A. Fielicke
Institut für Optik und Atomare Physik, Technische Universität Berlin
Hardenbergstraße 36, 10623 Berlin (Germany)
E-mail: fielicke@physik.tu-berlin.de

Supporting information and the ORCID identification number(s) for the author(s) of this article can be found under <http://dx.doi.org/10.1002/anie.201609766>.

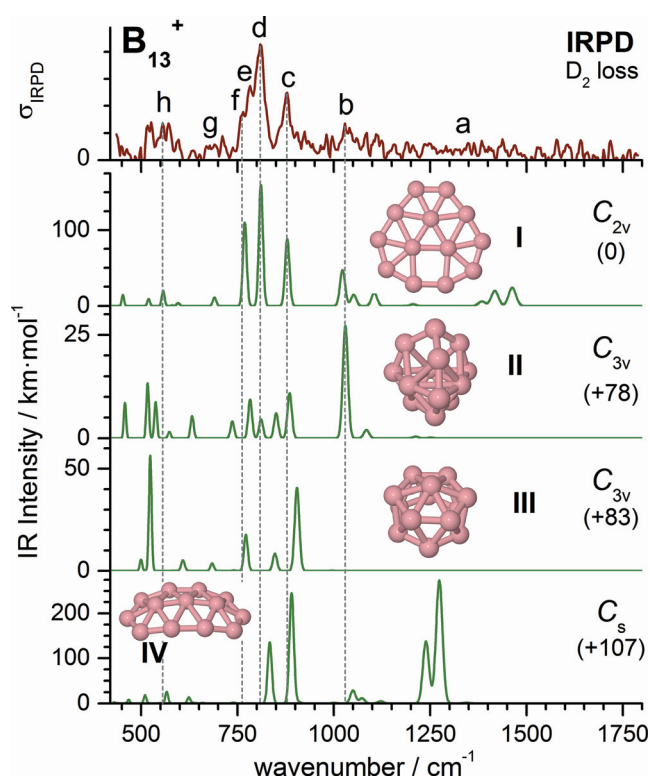


Figure 1. Comparison of the experimental IRPD spectrum of D_2 -tagged $^{11}B_{13}^+$ obtained by monitoring the D_2 -loss channel with four computed IR spectra of low-energy PBE0/TZVP minimum energy structures, derived from scaled (0.9575) harmonic frequencies and intensities, of bare $^{11}B_{13}^+$. TPSS/def2-TZVPP energies^[4b] (in $kJ \cdot mol^{-1}$), relative to that of bare $^{11}B_{13}^+$ are given in parentheses. Broken lines are shown to aid the eye and coincide with experimental band maxima listed in Table 1.

ously, but it should also contain characteristic signatures of its unusual fluxional behavior.

The gas-phase vibrational spectrum of B_{13}^+ , measured by way of infrared photodissociation (IRPD) spectroscopy of the messenger-tagged $^{11}B_{13}^+(D_2)$ complex, is shown in Figure 1. It

exhibits four bands at 1029 cm^{-1} (b), 878 cm^{-1} (c), 809 cm^{-1} (d) and 556 cm^{-1} (h). All bands appear substantially broader than the spectral bandwidth ($< 10 \text{ cm}^{-1}$). Band d, for example, extends from 750 to 830 cm^{-1} , and we therefore attribute the additional structure observed on its lower-energy side in the form of two peaks at 782 cm^{-1} (e) and 764 cm^{-1} (f) to additional, overlapping transitions. Weaker absorptions, close to the signal/noise ratio, are present at higher energies in-between 1200 and 1500 cm^{-1} (a) and centered around 700 cm^{-1} (g).

Also shown in Figure 1 are the computed harmonic IR spectra, derived from scaled harmonic frequencies and intensities (see Table 1), of four low-energy isomers (see Table S1 in the Supporting Information (SI) for Cartesian atomic coordinates), which were also considered in the previous ion mobility study.^[4b] These are the planar C_{2v} structure (I), now generally accepted as the global ground state, two 3D C_{3v} structures (II and III), computed 78 and 83 $kJ \cdot mol^{-1}$ higher in energy, respectively, as well as a quasi-planar C_s structure (IV, $+107 \text{ kJ} \cdot mol^{-1}$). Satisfactory agreement with the experimental spectrum is only found for the computed spectrum of the global ground state structure I, spectroscopically confirming its assignment. The IR spectra of isomers II–IV also show characteristic absorption bands in-between 750 – 900 cm^{-1} , but each of them exhibits its highest intensity transition (II: 1028 cm^{-1} , III: 523 cm^{-1} , IV: 1273 cm^{-1}) in a spectral region where there is no comparably intense signal in the experimental spectrum.

The vibrational normal modes of isomer I can be roughly classified into those that predominantly involve displacement of the atoms comprising either the outer B_{10} -ring or the inner B_3 -ring (see Table 1). The B–B stretching modes of the B_{10} -ring are found at highest energy ($> 1000 \text{ cm}^{-1}$) and have low IR intensity ($\leq 48 \text{ km} \cdot mol^{-1}$). The most intense B–B stretch transition is predicted at 1023 cm^{-1} (see Table 1) and is therefore assigned to band b. The higher energy modes (1206 – 1463 cm^{-1}) then contribute to the broad and weak absorptions associated with feature a. Band c is associated with the two

Table 1: Experimental IR band positions (in cm^{-1}), computed vibrational frequencies (in cm^{-1}) and intensities (in $km \cdot mol^{-1}$, in parenthesis) as well as tentative normal mode assignments. All computed normal modes above 700 cm^{-1} as well as those normal modes below 700 cm^{-1} involving the inner B_3 ring are listed.

Band	Expt.	Harmonic (PBE0/TZVP) ^[a]	Anharmonic(VPT2/PBE0/TZVP)	Assignment ^[b]
a	1200–1500	1463 (24), 1418 (20), 1384 (6), 1206 (2), 1185 (0) 1105 (17)	1492 (20), 1450 (14), 1419 (4), 1235 (1), 1220 (0) 1128 (13)	B–B stretches (B_{10} -ring) B_3 sym. stretch
b	1029	1051 (14), 1023 (47)	1086 (10), 1052 (31)	B–B stretches (B_{10} -ring)
c	878	881 (22), 879 (67)	898 (31), 897 (16)	B_3 asym. stretches
d	809	811 (160)	827 (129)	B_3 frust. translation (ip)
e	782	n/a	796 (22)	1 st overtone of B_3 frust. rotation (op) ^[c]
f	762	769 (110)	784 (63)	B_{10} -ring def. (ip)
g	711/690	690 (11)	713 (7)	B_3 frust. rotation (ip)/ B_{10} -ring def. (ip)
h	556	557 (19) 404 (0) 390 (0) 148 (14) 126 (10)	577 (9) 419 (0) 397 (0) 150 (12) 101 (8)	B_3 frust. translation (ip) B_3 frust. rotation (op) B_3 frust. rotation (op) B_3 frust. translation (op) B_{10} -ring def. (ip)/ B_3 frust. rotation (ip)

[a] Scaled by 0.9575 to account for anharmonic effects as well as systematic errors on the harmonic force constants (see SI for details). [b] Sym. (symmetric), asym. (antisymmetric), frust. (frustrated), def. (deformation), ip (in-plane), op (out-of-plane). [c] See Table S2 for other weaker transitions predicted in this spectral region.

antisymmetric stretching modes of the B_3 -ring predicted at 888 and 886 cm^{-1} . The corresponding B_3 symmetric stretch is computed at 1114 cm^{-1} with lower IR activity. The most intense IR band d as well as band h correspond to the excitation of the two in-plane frustrated translational modes of the B_3 -ring with harmonic intensities of 163 and 20 km mol^{-1} , respectively. The remaining (out-of-plane) frustrated translation mode is predicted much lower in energy at 148 cm^{-1} , outside of the accessible measurement window with the present experimental setup. Peak f is attributed to the highest energy B_{10} ring deformation mode and is the second most intense IR transition (112 km mol^{-1}). The normal mode associated with band g shows similar contributions from inner and outer atoms. It is one of two b_1 modes (the other is predicted at 133 cm^{-1}) that correspond to a combination of outer ring deformations with the B_3 in plane librational mode. This leaves peak e unassigned, which cannot be attributed to a fundamental harmonic mode of isomer **I** (see below).

While the harmonic spectrum of **I** reproduces the main absorption bands observed in the IRPD spectrum, it does not account for several of the weaker features, including the small but significant IR activity below 750 cm^{-1} as well as peak e. These may either be due to the perturbation from the messenger molecule or anharmonic effects, including those related to the predicted exceptional fluxionality of B_{13}^+ . To address the first point, we compare the harmonic spectra of bare B_{13}^+ to those of three $[B_{13}D_2]^+$ species in Figure 2. D_2 can in principle either be physisorbed or chemisorbed. This leads to the weakly bound top-on and side-on isomers with binding energies of 4 and 5 kJ mol^{-1} , respectively, and a covalently bound $B_{11}(BD)_2^+$ structure with a binding energy of 188 kJ mol^{-1} . From the two physisorbed D_2 -complexes, the top-on species leads to a nearly identical spectrum as that of bare B_{13}^+ (see Figure 2), while the spectrum of the side-on species does not agree as well with the experimental one. The computed spectrum of the species containing dissociatively adsorbed D_2 could indeed account for peak e. However, photodissociation of this species is not likely under the present experimental conditions (unfocused IR laser beam), considering the comparably low computed IR intensities ($\leq 163 \text{ km mol}^{-1}$), in combination with a high dissociation limit, which would require the absorption of more than ten IR photons. Moreover, its formation in the cold ion trap under thermalized conditions is probably kinetically inhibited.

To characterize static anharmonic effects we computed the anharmonic spectrum (see Figure 3 and Table 1) of structure **I** using vibrational perturbation theory (see SI). The main difference with respect to the corresponding harmonic spectrum is a slight broadening of most spectral features, particularly in the region of bands c, d and f, due to excitation of combination and overtone transitions. We then computed the harmonic spectrum associated with the first-order transition state (TS) for the in-plane rotation of the B_3 ring. Note, the TS lies only 0.4 kJ mol^{-1} above the minimum energy configuration (including zero-point energy correction),^[9a,c] leading to a vibrational ground state wavefunction with non-zero probability near the TS region for internal rotation. Compared to the spectrum of the global minimum energy structure **I**, the harmonic spectrum of the TS (see

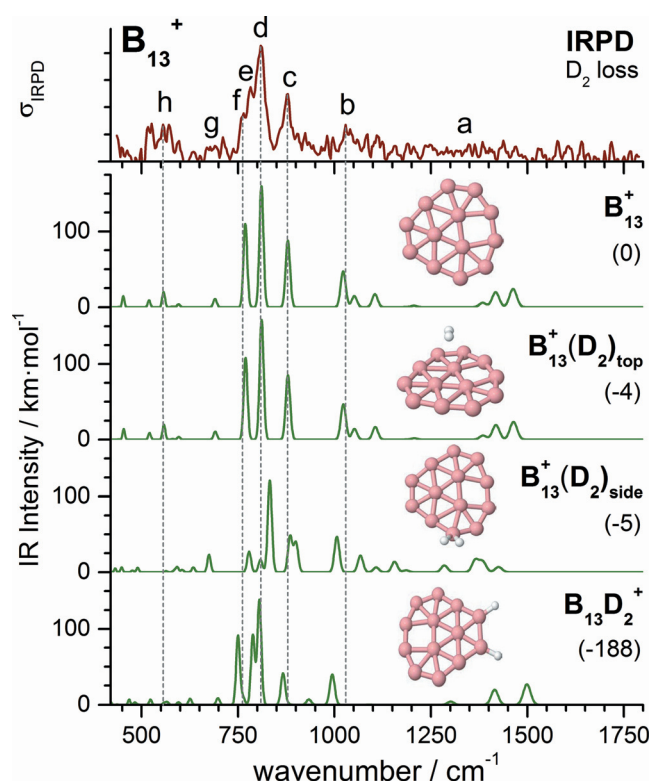


Figure 2. Comparison of the computed IR spectra, derived from PBE0/TZVP scaled (0.9575) harmonic frequencies and intensities of bare and D_2 -tagged $^{11}B_{13}^+$. The top and side isomers of $^{11}B_{13}^+(D_2)$ as well as a covalently bound $^{11}B_{13}D_2^+$ isomer are shown. D_2 binding energies (in kJ mol^{-1}) are given in parentheses. Broken lines are shown to aid the eye and coincide with experimental band maxima listed in Table 1.

Figure 3) is characterized by a blue-shifted outer-ring in-plane deformation mode at 778 cm^{-1} (vs. 769 cm^{-1}), which can account for the additional signal in-between peaks d (809 cm^{-1}) and f (762 cm^{-1}). Hence, this provides a first evidence that peak e (782 cm^{-1}) can be associated with the internal quasi-rotation of the B_3 moiety in B_{13}^+ .

That internal quasi-rotation is the origin of these rather subtle effects observed in the IRPD spectrum is further corroborated by the results of BOMD simulations (see SI for details) performed at 100, 300 and 600 K. The corresponding BOMD vibrational spectra are shown in the bottom panels of Figure 3 and include both static and dynamic anharmonic effects. Indeed, we observe a motion of both rings with a rate of 20 GHz (100 K), 80 GHz (300 K) and 220 GHz (600 K) (see Figure S2 in the SI). Note, the BOMD simulation temperature is not a justified thermodynamic quantity for such a small molecule and should rather be considered as a measure of the internal kinetic energy. Inspecting the evolution of the BOMD vibrational signature with increasing temperature reveals a consistent picture of the fluxionality of B_{13}^+ : we observe a broadening of all spectral features, in particular of bands a, b, g and h, which is comparable to that observed in the experimental IRPD spectrum. Moreover, the computed intensity of band g, which is attributed to the in-plane B_3 frustrated rotation (see Table 1), decreases with increasing temperature, that is, it decreases due to the thermal activation of the mutual quasi-rotation between inner and

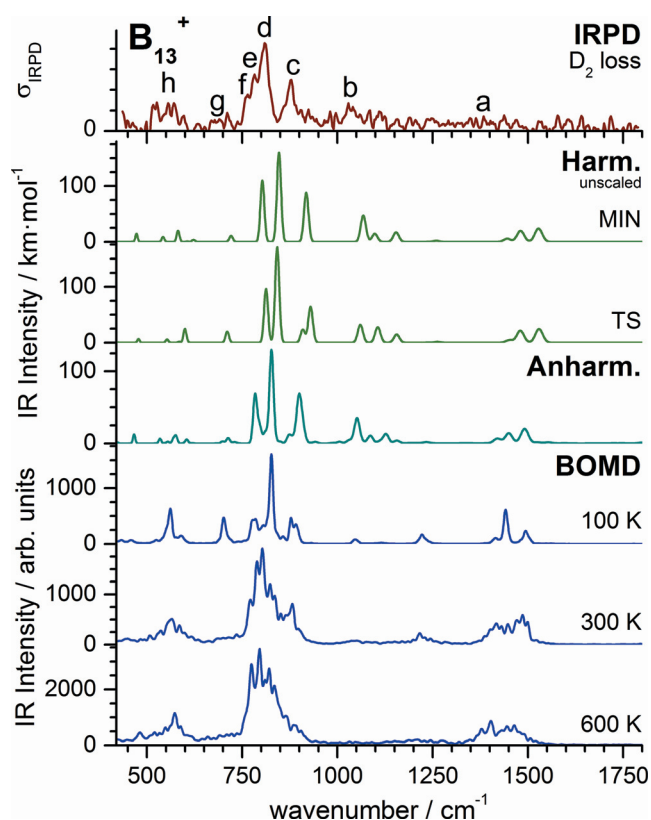


Figure 3. Comparison of computed IR spectra of bare $^{11}\text{B}_{13}^+$, derived either from PBE0/TZVP harmonic frequencies and intensities of the global minimum energy structure I (MIN) and the first order transition state (TS), VPT2/PBE0/TZVP anharmonic frequencies and intensities of I or from BOMD simulations (PBE/DZVP, for comparison of both levels see Figure S1 in SI) performed at 100 K, 300 K and 600 K, respectively.

outer ring. Band e is also reproduced by the BOMD spectra and its intensity increases with temperature, eventually forming a wide feature comprising bands c, d, e and f. Analysis of the BOMD trajectories finally reveals that bands e and g are directly related to the large amplitude motion involving the unhindered internal quasi-rotation of the B_3 moiety of a planar concentric double ring structure. Note, no fluxionality is found for the related neutral B_{12} cluster that has one boron atom less in the outer ring.^[12] Consequently, static and BOMD calculations yield similar IR spectra and in particular no “disappearing” bands are observed in the BOMD spectra at elevated temperatures (see Figure S3).

The highly fluxional character of B_{13}^+ discussed here illustrates a peculiar dynamical behavior, which goes substantially beyond the typical conformational dynamics observed within weakly bound van-der-Waals complexes and hydrogen-bonded clusters. It is also characteristically different from that previously described in strongly bound clusters like Au_7^+ or Si_{16}V^+ .^[13] Here, the inherent fluxionality of B_{13}^+ is directly linked to its aromaticity, that is, its delocalized bonding, resulting in the absence of any localized bonds between the inner B_3 - and outer B_{10} -ring. Consequently, internal rotation does not require the formal breaking and reformation of any covalent bonds in this case. The identification and characterization of such special bonding

situations may ultimately prove quite helpful in the conception and design of new materials with tailored properties. Finally, our study also demonstrates that molecular stability does not demand structural rigidity.

Acknowledgements

This work has been supported by Deutsche Forschungsgemeinschaft within the Collaborative Research Center SFB 1109 and by a DFG research grant (FI 893/4). X.S. thanks the Alexander von Humboldt Foundation for a post-doctoral research fellowship. ZIH Dresden is gratefully acknowledged for providing high-performance computing resources.

Keywords: anharmonic effects · boron clusters · infrared photodissociation spectroscopy · internal rotation · molecular dynamics simulations

How to cite: *Angew. Chem. Int. Ed.* **2017**, *56*, 501–504
Angew. Chem. **2017**, *129*, 515–519

- [1] B. Albert, H. Hillebrecht, *Angew. Chem. Int. Ed.* **2009**, *48*, 8640–8668; *Angew. Chem.* **2009**, *121*, 8794–8824.
- [2] I. Boustani, A. Quandt, E. Hernandez, A. Rubio, *J. Chem. Phys.* **1999**, *110*, 3176–3185.
- [3] a) D. Ciuparu, R. F. Klie, Y. M. Zhu, L. Pfefferle, *J. Phys. Chem. B* **2004**, *108*, 3967–3969; b) F. Liu, C. M. Shen, Z. J. Su, X. L. Ding, S. Z. Deng, J. Chen, N. S. Xu, H. J. Gao, *J. Mater. Chem.* **2010**, *20*, 2197–2205.
- [4] a) A. P. Sergeeva, I. A. Popov, Z. A. Piazza, W.-L. Li, C. Romanescu, L.-S. Wang, A. I. Boldyrev, *Accs. Chem. Res.* **2014**, *47*, 1349–1358; b) E. Oger, N. R. M. Crawford, R. Kelting, P. Weis, M. M. Kappes, R. Ahlrichs, *Angew. Chem. Int. Ed.* **2007**, *46*, 8503–8506; *Angew. Chem.* **2007**, *119*, 8656–8659; c) Q. Chen, W.-L. Li, Y.-F. Zhao, S.-Y. Zhang, H.-S. Hu, H. Bai, H.-R. Li, W.-J. Tian, H.-G. Lu, H.-J. Zhai, S.-D. Li, J. Li, L.-S. Wang, *ACS Nano* **2015**, *9*, 754–760.
- [5] L. Hanley, J. L. Whitten, S. L. Anderson, *J. Phys. Chem.* **1988**, *92*, 5803–5812.
- [6] A. Ricca, C. W. Bauschlicher, *Chem. Phys.* **1996**, *208*, 233–242.
- [7] J. E. Fowler, J. M. Ugalde, *J. Phys. Chem. A* **2000**, *104*, 397–403.
- [8] A. N. Alexandrova, A. I. Boldyrev, H.-J. Zhai, L.-S. Wang, *Coord. Chem. Rev.* **2006**, *250*, 2811–2866.
- [9] a) G. Martínez-Guajardo, A. P. Sergeeva, A. I. Boldyrev, T. Heine, J. M. Ugalde, G. Merino, *Chem. Commun.* **2011**, *47*, 6242–6244; b) J. Zhang, A. P. Sergeeva, M. Sparta, A. N. Alexandrova, *Angew. Chem. Int. Ed.* **2012**, *51*, 8512–8515; *Angew. Chem.* **2012**, *124*, 8640–8643; c) G. Merino, T. Heine, *Angew. Chem. Int. Ed.* **2012**, *51*, 10226–10227; *Angew. Chem.* **2012**, *124*, 10372–10373.
- [10] H.-J. Zhai, Y.-F. Zhao, W.-L. Li, Q. Chen, H. Bai, H.-S. Hu, Z. A. Piazza, W.-J. Tian, H.-G. Lu, Y.-B. Wu, Y.-W. Mu, G.-F. Wei, Z.-P. Liu, J. Li, S.-D. Li, L.-S. Wang, *Nat. Chem.* **2014**, *6*, 727–731.
- [11] C. Romanescu, D. J. Harding, A. Fielicke, L.-S. Wang, *J. Chem. Phys.* **2012**, *137*, 014317.
- [12] L. Liu, D. Moreno, E. Osorio, A. C. Castro, S. Pan, P. K. Chattaraj, T. Heine, G. Merino, *RSC Adv.* **2016**, *6*, 27177–27182.
- [13] a) L. M. Ghiringhelli, P. Gruene, J. T. Lyon, D. M. Rayner, G. Meijer, A. Fielicke, M. Scheffler, *New J. Phys.* **2013**, *15*, 083003; b) P. Claes, E. Janssens, V. T. Ngan, P. Gruene, J. T. Lyon, D. J. Harding, A. Fielicke, M. T. Nguyen, P. Lievens, *Phys. Rev. Lett.* **2011**, *107*, 173401.

Manuscript received: October 5, 2016

Final Article published: December 5, 2016